Biomedical Optics EXPRESS

Three-dimensional, non-invasive, cross-sectional imaging of protein crystals using ultrahigh resolution optical coherence tomography

Norihiko Nishizawa,[1,5] Shutaro Ishida,[1] Mika Hirose,[2] Shigeru Sugiyama,[3] Tsuyoshi Inoue,[2] Yusuke Mori,[3] Kazuyoshi Itoh,[4] and Hiroyoshi Matsumura[2,6]

[1]*Dept. Electrical Engineering and Computer Science, Nagoya University, Nagoya, 464-8603, Japan*
[2]*Dept. Applied Chemistry, Graduate School of Engineering, Osaka University, Japan*
[3]*Dept. Electrical Engineering, Graduate School of Engineering, Osaka University, Japan*
[4] *Div. Advanced Science and Biotechnology, Osaka University, Japan*
[5]*nishizawa@nuee.nagoya-u.ac.jp*
[6]*matsumura@chem.eng.osaka-u.ac.jp*

Abstract: Micro-scale, non-invasive, three-dimensional cross-sectional imaging of protein crystals was successfully accomplished using ultra-high resolution optical coherence tomography (UHR-OCT) with low noise, Gaussian like supercontinuum. This technique facilitated visualization of protein crystals even those in medium that also contained substantial amounts of precipitates. We found the enhancement of the scattered signal from protein crystal by inclusion of agarose gel in the crystallization medium. Crystals of a protein and a salt in the same sample when visualized by UHR-OCT showed distinct physical characteristics, suggesting that protein and salt crystals may, in general, be distinguishable by UHR-OCT. UHR-OCT is a nondestructive and rapid method, which should therefore find use in automated systems designed to visualize crystals.

OCIS codes: (110.4500) Optical coherence tomography; (170.3880) Medical and biological imaging.

References and links

1. R. A. Judge, K. Swift, and C. González, "An ultraviolet fluorescence-based method for identifying and distinguishing protein crystals," Acta Crystallogr. D Biol. Crystallogr. **61**(1), 60–66 (2005).
2. J. J. Kehoe, G. E. Remondetto, M. Subirade, E. R. Morris, and A. Brodkorb, "Tryptophan-mediated denaturation of beta-lactoglobulin A by UV irradiation," J. Agric. Food Chem. **56**(12), 4720–4725 (2008).
3. D. Huang, E. A. Swanson, C. P. Lin, J. S. Schuman, W. G. Stinson, W. Chang, M. R. Hee, T. Flotte, K. Gregory, C. A. Puliafito, and J. G. Fujimoto, "Optical coherence tomography," Science **254**(5035), 1178–1181 (1991).
4. B. E. Bouma and G. J. Tearney, *Handbook of Optical Coherence Tomography* (Marcel Dekker, 2002)
5. W. Drexler and J. G. Fujimoto, *Optical Coherence Tomography* (Springer, 2008).
6. J. P. Dunkers, R. S. Parnas, C. G. Zimba, R. S. Peterson, K. M. Flynn, J. G. Fujimoto, and B. E. Bouma, "Optical coherence tomography of glass reinforced polymer composites," Compos., Part A Appl. Sci. Manuf. **30**, 139–145 (1999).
7. C. Biertümpfel, J. Basquin, D. Suck, and C. Sauter, "Crystallization of biological macromolecules using agarose gel," Acta Crystallogr. D Biol. Crystallogr. **58**(10), 1657–1659 (2002).
8. B. Lorber, C. Sauter, M. C. Robert, B. Capelle, and R. Giegé, "Crystallization within agarose gel in microgravity improves the quality of thaumatin crystals," Acta Crystallogr. D Biol. Crystallogr. **55**(9), 1491–1494 (1999).
9. S. Sugiyama, H. Hasenaka, M. Hirose, N. Shimizu, T. Kitatani, Y. Takahashi, H. Adachi, K. Takano, S. Murakami, T. Inoue, Y. Mori, and H. Matsumura, "Femtosecond laser processing of Agarose gel surrounding protein crystals for development of an automated Crystal capturing system," Jpn. J. Appl. Phys. **48**(10), 105502 (2009).
10. H. Hasenaka, S. Sugiyama, M. Hirose, N. Shimizu, T. Kitatani, Y. Takahashi, H. Adachi, K. Takano, S. Murakami, T. Inoue, Y. Mori, and H. Matsumura, "Femtosecond laser processing of protein crystals grown in agarose gel," J. Cryst. Growth **312**(1), 73–78 (2009).
11. S. Sugiyama, M. Hirose, N. Shimizu, M. Niiyama, M. Maruyama, G. Sazaki, R. Murai, H. Adachi, K. Takano, S. Murakami, T. Inoue, Y. Mori, and H. Matsumura, "Effect of evaporation on protein crystals grown in semi-solid agarose hydrogel," Jpn. J. Appl. Phys. **50**(2), 025502 (2011).
12. C. Sauter, B. Lorber, and R. Giegé, "Towards atomic resolution with crystals grown in gel: the case of thaumatin seen at room temperature," Proteins **48**(2), 146–150 (2002).

#162627 - $15.00 USD Received 7 Feb 2012; revised 14 Mar 2012; accepted 14 Mar 2012; published 15 Mar 2012

13. K. Tanabe, M. Hirose, R. Murai, S. Sugiyama, N. Shimizu, M. Maruyama, Y. Takahashi, H. Adachi, K. Takano, S. Murakami, Y. Mori, E. Mizohata, T. Inoue, and H. Matsumura, "Promotion of crystal nucleation of protein by semi-solid Agarose gel," Appl. Phys. Express **2**(12), 125501 (2009).
14. K. J. Thiessen, "The use of two novel methods to grow protein crystals by microdialysis and vapor diffusion in an agarose gel," Acta Crystallogr. D Biol. Crystallogr. **50**(4), 491–495 (1994).
15. W. Drexler, U. Morgner, R. K. Ghanta, F. X. Kärtner, J. S. Schuman, and J. G. Fujimoto, "Ultrahigh-resolution ophthalmic optical coherence tomography," Nat. Med. **7**(4), 502–507 (2001).
16. J. G. Fujimoto, A. D. Aguirre, Y. Chen, P. R. Herz, P.-L. Hsiung, T. H. Ko, N. Nishizawa, and F. X. Kartner, *Ultrashort Laser Pulses in Biology and Medicine* (Springer, 2007), Chap. 1.
17. M. Nishiura, T. Kobayashi, M. Adachi, J. Nakanishi, T. Ueno, Y. Ito, and N. Nishizawa, "In vivo ultrahigh-resolution ophthalmic optical coherence tomography using Gaussian-shaped super continuum," Jpn. J. Appl. Phys. **49**(1), 012701 (2010).
18. S. Ishida and N. Nishizawa, "Quantitative comparison of contrast and imaging depth of ultrahigh-resolution optical coherence tomography images in 800-1700 nm wavelength region," Biomed. Opt. Express **3**(2), 282–294 (2012).
19. D. Kobayashi, M. Tamoi, T. Iwaki, S. Shigeoka, and A. Wadano, "Molecular characterization and redox regulation of phosphoribulokinase from the cyanobacterium *Synechococcus sp*. PCC 7942," Plant Cell Physiol. **44**(3), 269–276 (2003).
20. A. Wadano, Y. Kamata, T. Iwaki, K. Nishikawa, and T. Hirahashi, "Purification and characterization of phosphoribulokinase from the cyanobacterium *Synechococcus* PCC7942," Plant Cell Physiol. **36**(7), 1381–1385 (1995).
21. J. A. Gavira and J. M. García-Ruiz, "Agarose as crystallisation media for proteins II: trapping of gel fibres into the crystals," Acta Crystallogr. D Biol. Crystallogr. **58**(10), 1653–1656 (2002).
22. S. Sugiyama, K. Tanabe, M. Hirose, T. Kitatani, H. Hasenaka, Y. Takahashi, H. Adachi, K. Takano, S. Murakami, Y. Mori, T. Inoue, and H. Matsumura, "Protein crystallization in Agarose gel with high strength: developing an automated system for protein crystallographic processes," Jpn. J. Appl. Phys. **48**(7), 075502 (2009).
23. N. Pernodet, M. Maaloum, and B. Tinland, "Pore size of agarose gels by atomic force microscopy," Electrophoresis **18**(1), 55–58 (1997).

1. Introduction

X-ray crystallography is used to determine three-dimensional structures of proteins at atomic resolution. Protein crystals are required for this method, and automated robotic systems are currently used to prepare many different test media so that crystallization conditions can be rapidly surveyed. However, three dimensional imaging, which is important for automated treatment of protein crystal, is generally difficult by light microscopy. In addition, the crystals in these media are frequently difficult to identify by conventional light microscopy because the media often also contain salt crystals, e.g., NaCl, that appear similar to protein crystals, and/or protein crystals that are not suitable for X-ray crystallography, and/or amorphous materials that obscure the presence of usable protein crystals. Consequently, ultraviolet microscopy has been used to identify protein crystals [1]; however, ultraviolet light can damage proteins [2].

Optical coherence tomography (OCT) is an emerging technique for μm-scale cross-sectional imaging [3–5]. Generally, the axial resolution obtainable by OCT is ~10 μm and is dependent on the center wavelength and bandwidth of the light source. OCT is a non-destructive, rapid, three-dimensional imaging tool that has been used to visualize biological tissues and other materials. OCT has received much attention especially for medical imaging, and it has been used in ophthalmology clinics, etc. [3–5]. The application for industrial field, such as the investigation of polymer matrix composites, has also been demonstrated [4,6]. The OCT signal is a beam backscattered from the sample, which makes the visualization of nearly transparent and low-scattering samples difficult.

Agarose gels have been included in protein crystallization media as they reduce solvent convection and prevent crystal sedimentation, which allows protein crystals to grow as if under microgravity [7,8]. When protein crystals are grown in agarose gels, they become trapped in the pores of the gel matrix. By immobilizing the crystals in a gel, the crystals can be subjected to processed by a femtosecond laser irradiation to mount onto the X-ray diffraction equipment for data collection [9,10]. Such crystals are more resistant to environmental perturbations, e.g., evaporation [11] and osmotic shock [12]. Furthermore, agarose gels promote protein nucleation [13,14].

#162627 - $15.00 USD Received 7 Feb 2012; revised 14 Mar 2012; accepted 14 Mar 2012; published 15 Mar 2012

Herein we report the first micro-scale, non-invasive, three-dimensional cross-sectional images of protein crystals by ultra-high resolution (UHR) OCT [15,16]. In the developed UHR-OCT, the axial resolution of 2 μm in sample was achieved using a broadband supercontinuum (SC) source and specially optimized OCT at 800 nm wavelength region [17,18]. As mentioned above, OCT cannot detect transparent objects, e.g., ideal crystals, because such crystals have homogeneous nano-structures for which the scattering coefficient is small. As we report below, as expected, the OCT signal intensities of protein crystals that had been grown in solution were extremely small. Additionally, we found that the backscattered signals of protein crystals were enhanced when the crystals were grown in agarose gel-containing medium. Even when the crystallization medium contained substantial amounts of precipitants, such that the protein crystals could not been clearly seen by light microscopy, they were easily detectable by UHR-OCT. Finally, we found that the UHR-OCT images of salt and protein crystals differed, suggesting that the two types of crystals may routinely be differentiated by UHR-OCT

2. Methods and Materials

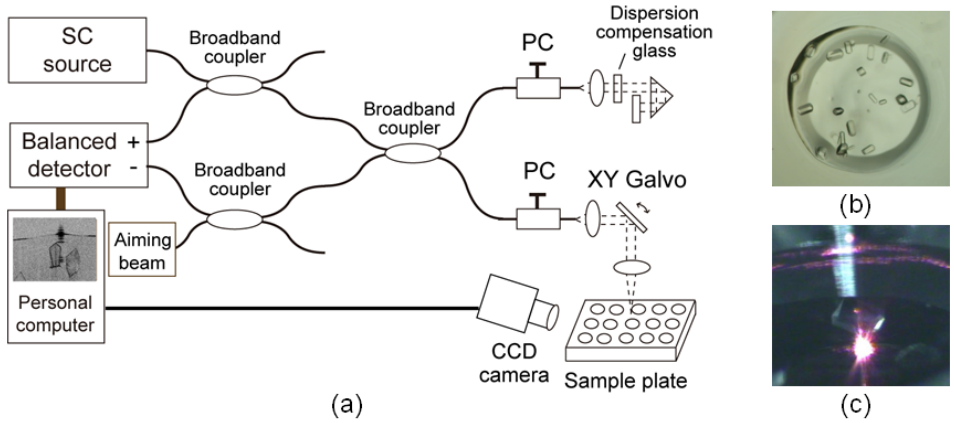

Fig. 1. (a) Experimental setup of 3D imaging of protein crystals using UHR-OCT with SC, (b) example of light micrograph of protein crystals, (c) example of picture of protein crystal taken with CCD camera when the aiming beam was irradiated. SC: supercontinuum, PC: polarization controller.

Figure 1(a) shows the experimental setup and pictures of protein crystals. A time-domain UHR-OCT system was constructed that simultaneously produces ultrahigh resolution and large-depth imaging. The axial resolution of OCT is determined by the center wavelength and bandwidth of the light source [4,5]. We used a 100-fs ultrashort pulse centered at 800 nm from a Ti:sapphire laser, which were coupled to a normal dispersive polarization-maintaining fiber (PMF) after dispersion compensation through a pair of prisms. A low noise, 350 mW, Gaussian-shaped, wideband SC with a bandwidth of 120 nm at full width at half-maximum was generated [17,18]. The corresponding theoretical axial resolution was 2.9 μm in air and 2.1 μm in water. The SC was attenuated by a spatial fiber coupler and then introduced into a fiber interferometer. The SC was split into signal and reference beams by a broadband fiber coupler. The optical path length of the reference beam was scanned using a corner-cube prism mounted on a galvanometer. The signal beam was spatially scanned using an XY galvanometer-based scanning probe and next automated imaging was performed. The small backscattered signal was combined with the reference beam at the broadband fiber coupler so that only the interference signal was collected at the balanced detector. The system sensitivity was 95 dB with the signal beam power of 3 mW on the sample.

The interference signal was transferred to a personal computer to construct cross-sectional images. The cross-sectional image consists of 250 transverse scans with 1000 pixels per scan,

#162627 - $15.00 USD Received 7 Feb 2012; revised 14 Mar 2012; accepted 14 Mar 2012; published 15 Mar 2012

covering an area of 2.0 mm by 1.0 mm. The imaging speed was 1 frame per second. The lateral resolution was 17.6 μm. For the imaging of protein crystals, the visible aiming beam was combined with SC and used to know the beam irradiation point. A CCD camera with zooming lens was also used to monitor the observation point on the sample (Fig. 1(c)).

Figure 1(b) shows a picture of protein crystals in a sample plate. For the preparation of protein crystals, Hen egg white lysozyme (HEWL, Seikagaku Corporation), agarose IX-A (Sigma-Aldrich), and 96-well microbatch plates (Hampton Research) were mainly used for crystallization [10]. HEWL (50 mg/ml) was crystallized by the batch method at 293 K in 0.33 M sodium acetate, 0.033 M sodium acetate (pH 4.5), 0.51 M sodium chloride, and agarose at 0.4% (w/v) increments between 0% and 2.0% (w/v) [13]. To prepare HEWL crystals in the substantial amounts of precipitants, HEWL (10 mg/ml) was crystallized in 0.25 M calcium chloride, 0.1 M citrate acetate, 0.066 M sodium acetate (pH 4.5), 0.85 M sodium chloride, 1.6% (w/v) agarose. To obtain salt and protein crystals simultaneously, the HEWL (12 mg/ml) was crystallized in 0.05 M calcium chloride, 0.1 M potassium phosphate, 0.066 M sodium acetate (pH 4.5), 0.85 M sodium chloride, 2.0% (w/v) agarose.

For comparison, *Synechococcus* phosphoribulokinase was purified as described [19] and crystallized by the sitting-drop method in 0.1 M 2-N-morpholino-ethanesulfonic acid buffer (pH 6.5), 10% (w/v) isopropanol, 0.2 M potassium acetate, 1% (w/v) agarose at 293 K.

3. Results and Discussion

We first used UHR-OCT to visualize the HEWL protein crystals grown in the presence of the different agarose concentrations to ascertain how the agarose gel affected the UHR-OCT images (Fig. 2). The positions of HEWL crystals and aiming beam were observed by CCD camera as shown in Fig. 1(c). When agarose was absent, crystals were hardly visible, probably because of their small backscattered signals (Fig. 2(a)). The backscattered signals were enhanced as the agarose concentration was increased (Fig. 2(a-e)), so that the crystals grown in the presence of 1.8% (w/v) agarose were clearly visible. The backscattered signals associated with the edges of the crystals were greatly enhanced (10-28 dB above the noise floor for the 1.8% agarose sample), which resulted in clear crystal profiles (Fig. 2(e)). The presence of the agarose gel therefore effectively enhanced the backscattered signals of the protein crystals. The average values for the backscattered signals for gel-grown HEWL crystals, agarose-gel-containing medium around the HEWL crystals, and solution-grown HEWL crystals were ~5, 2, and 0 dB above the noise floor, respectively. The standard deviation was 3 dB for a thousand sampling points in each part. We examined three sample plates of HEWL crystals and they showed almost the same results.

We also used crystallized *Synechococcus* phosphoribulokinase as a test case [19,20]. The crystals were clearly visualized by UHR-OCT (Fig. 2(f)). Therefore, in general, agarose gels may enhance the backscattered signal, which would facilitate protein crystal visualization. Probably, the signal enhancement is a consequence of the different protein and agarose medium refractive indexes. As mentioned above, OCT signals are back-scattered at the boundaries of materials with distinct refractive indexes [4,5]. Agarose fibers penetrate protein crystals [21,22], suggesting that many boundaries between protein molecules and agarose fibers exist within the crystals, which would increase the intensity of the OCT signals.

According to the Rayleigh-scattering theorem, the scattering coefficient is proportional to d^6/λ^4, where d is the diameter of the scattering particles and λ is the wavelength of the irradiation beam. When protein crystals are grown in an agarose gel, the protein molecules are captured within the agarose-gel pores, which are ~300 nm in diameter [23]. Consequently, the protein molecules behave as small particles with diameters of a few hundred nm, which enhance the Rayleigh scattering signal.

Clinically, OCT is currently used to image semitransparent organs, e.g., the human eye, and practically opaque organs, e.g., human skin, internal organs, and blood vessels [3], which suggested to us that UHR-OCT could be used to visualize proteins that had been grown in agarose-gel-containing medium that also contained substantial amounts of opaque precipitants. Notably, visualization of crystals by light microscopy is difficult when the

#162627 - $15.00 USD Received 7 Feb 2012; revised 14 Mar 2012; accepted 14 Mar 2012; published 15 Mar 2012

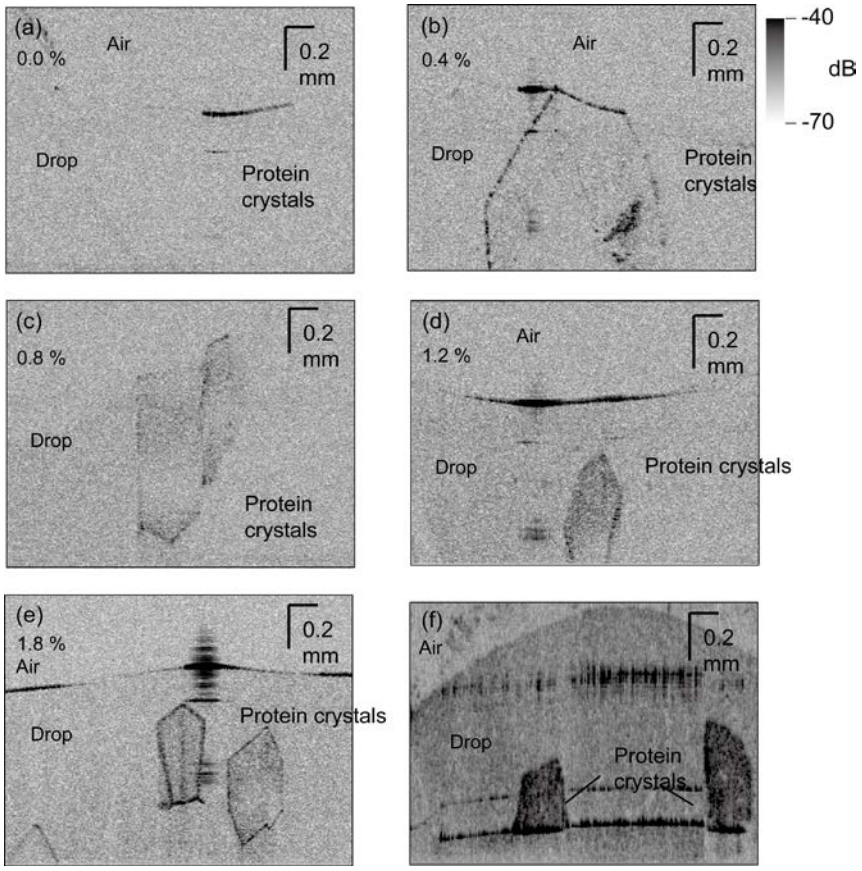

Fig. 2. Cross sections of three-dimensional UHR-OCT images of HEWL crystals grown in (a) 0.0, (b) 0.4, (c) 0.8, (d) 1.2, and (e) 1.8% (w/v) agarose. (f) An image of a drop that contained *Synechococcus* phosphoribulokinase crystals and 1.0% (w/v) agarose. The crystals shown in panels (e) and (f) are clearly and non-invasively seen at μm resolution. Media 1 shows the 3D UHR-OCT image of HEWL crystals grown in the same condition as that for Fig. 2(e).

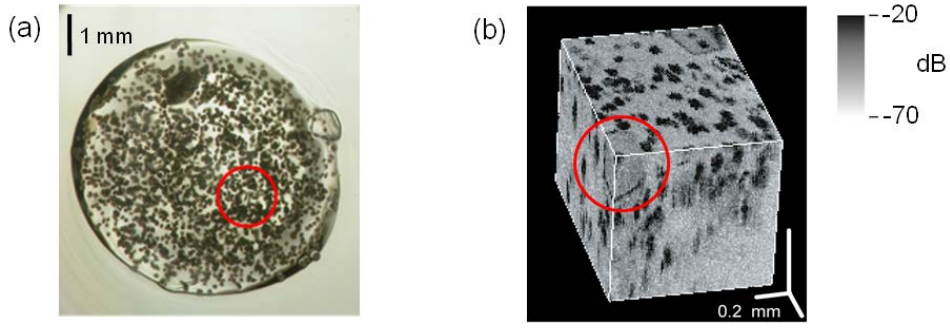

Fig. 3. (a) Light micrograph. The HEWL crystal, circled in red, is difficult to see because it is surrounded by aggregates and amorphous material. (b) Cross section of a three-dimensional UHR-OCT image. The protein crystal is circled in red. The aggregates and amorphous material are colored black. The cross section is a still from Media 2.

medium also contains a large amount of precipitant. To test our hypothesis, HEWL in the substantial amounts of precipitants was used as the sample. Indeed, identification of the HEWL crystals by light microscopy was difficult (Fig. 3(a)), whereas the well-shaped HEWL

#162627 - $15.00 USD Received 7 Feb 2012; revised 14 Mar 2012; accepted 14 Mar 2012; published 15 Mar 2012

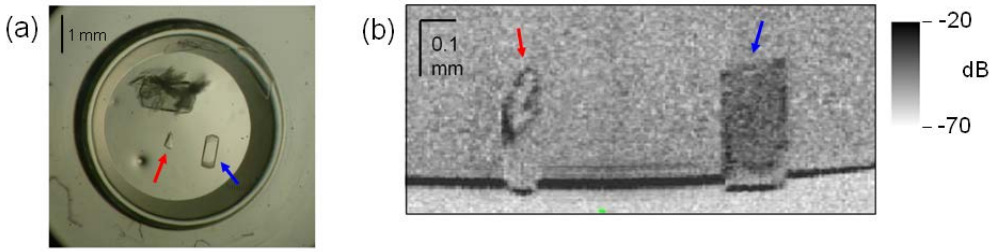

Fig. 4. (a) Light micrograph. Differentiating between the HEWL crystal and the calcium phosphate crystal is difficult. (b) Cross section of a three-dimensional UHR-OCT image. The red arrow points the calcium phosphate crystal and the blue arrow points the HEWL crystal. The difference in the signal intensities provides a better means of differentiating between the HEWL crystal and the calcium phosphate crystal. Media 3 shows the 3D UHR-OCT image of HEWL crystals and the calcium phosphate crystal.

crystals were clearly detected by UHR-OCT (Fig. 3(b)). UHR-OCT may therefore be a powerful tool for detecting protein crystals in medium containing precipitants.

Finally, we tested the ability of UHR-OCT to discriminate between salt and protein crystals. As shown in Fig. 4(a), both potassium phosphate and HEWL crystals were grown under this condition. Two types of crystals with different shapes were found (Fig. 4). Using X-ray diffraction, the crystal on the left in Fig. 4(a) was identified as calcium phosphate and the one on the right as an HEWL crystal. Light microscopy could only discern the size and shape of the two crystals (Fig. 4(a)). Conversely, additional characteristic differences for the two crystals were seen in their UHR-OCT images (Fig. 4(b)). The edges of the calcium phosphate crystal are enhanced by the UHR-OCT signals, but the crystal interior is nearly transparent owing to an absence of backscattered signals. Conversely, the UHR-OCT signals were enhanced both at the edges and the interior of the HEWL crystal, which allowed us to distinguish between the calcium phosphate and HEWL crystals. The averaged signal intensity from the interior of HEWL crystal was 10 dB higher than that of calcium phosphate crystal. The standard deviation was 4 dB. Probably the difference in the appearance of the crystals was caused by their different interior nano-structures. As described above, agarose fibers were present within HEWL crystals, but a previous study had not found agarose fibers within salt crystals [21]. Therefore, the salt-crystal interior should not backscatter light, whereas that of the protein would.

4. Conclusion

In conclusion, micro-scale, non-invasive, three-dimensional cross-sectional imaging of protein crystals was demonstrated for the first time using ultra-high resolution optical coherence tomography (UHR-OCT) with Gaussian supercontinuum. The protein crystals grown in the presence of the different agarose gel concentrations were examined, and the enhancement of the scattered signal from protein crystal by inclusion of agarose gel was confirmed. Using the UHR-OCT and agarose gel inclusion technique, the protein crystals could be visible, even when the crystallization medium contains substantial amounts of precipitants. The signals intensities from a protein and a salt crystals were obviously different, suggesting that protein and salt crystals may be distinguishable. UHR-OCT is a nondestructive and rapid method (several sec/sample in principle), which can be incorporated into a robotic system that can rapidly screen for protein crystals suitable for X-ray crystallography.

#162627 - $15.00 USD Received 7 Feb 2012; revised 14 Mar 2012; accepted 14 Mar 2012; published 15 Mar 2012